

# Hierarchical DWR Error Estimates for the Navier Stokes Equation: $h$ and $p$ Enrichment

B. Endtmayer<sup>1</sup>, U. Langer<sup>1</sup>, J. P. Thiele<sup>2</sup>, and T. Wick<sup>2</sup>

<sup>1</sup>Johann Radon Institute for Computational and Applied Mathematics, Austrian Academy of Sciences, Altenbergerstr. 69, A-4040 Linz, Austria

<sup>2</sup>Institut für Angewandte Mathematik, Leibniz Universität Hannover, Welfengarten 1, 30167 Hannover, Germany

## Abstract

In this work, we further develop multigoal-oriented a posteriori error estimation for the nonlinear, stationary, incompressible Navier-Stokes equations. It is an extension of our previous work [B. Endtmayer, U. Langer, T. Wick: Two-side a posteriori error estimates for the DWR method, *SISC*, 2019, accepted]. We now focus on  $h$  mesh refinement and  $p$  enrichment for the error estimator. These advancements are demonstrated with the help of a numerical example.

## 1 Introduction

Multigoal-oriented error estimation offers the opportunity to control several quantities of interest simultaneously. In recent years, we have developed a version [3, 4] which relies on the dual-weighted residual method [2], and also balances the discretization error with the nonlinear iteration error [12]. The localization is based on the weak formulation proposed in [13]. Our method uses on hierarchical finite element spaces. Here, we investigate  $h$  refinement along with  $p$  refinement to generate enriched spaces. These ideas are applied to the stationary incompressible Navier-Stokes equations. It is well-known that the spaces for the velocities and the pressure must be balanced in order to satisfy an inf-sup condition [6]. These requirements must be reflected in the design of the adjoint problems in dual-weighted residual error estimation and our proposed  $p$  refinement. To demonstrate the performance of the error estimator, we adopt the 2D-1 fluid flow benchmark [14].

## 2 The Model Problem and Discretization

### 2.1 The Model Problem

We consider the stationary Navier Stokes 2D-1 benchmark problem [14] as our model problem. This configuration was also considered in [4]. The domain  $\Omega \subset \mathbb{R}^2$  is given by  $(0, 2.2) \times (0, H) \setminus B$ , and  $B$  is the ball with the center  $(0.2, 0.2)$  and the radius 0.05 as given in [14] and visualized in Figure 1. Find  $\vec{u} = (u, p)$  such that

$$\begin{aligned} -\operatorname{div}(\nu(\nabla u + \nabla u^T)) + (u \cdot \nabla)u - \nabla p &= 0, & \text{in } \Omega, \\ -\operatorname{div}(u) &= 0, & \text{in } \Omega, \\ u &= u_{\text{in}} & \text{on } \Gamma_{\text{in}}, \\ u &= 0 & \text{on } \Gamma_{\text{no-slip}}, \\ \nu(\nabla u + \nabla u^T)\vec{n} + p\vec{n} &= 0 & \text{on } \Gamma_{\text{out}}, \end{aligned}$$

where  $\Gamma_{\text{in}} := \{x = 0\} \cap \partial\Omega$ ,  $\Gamma_{\text{no-slip}} := \overline{\partial\Omega \setminus (\Gamma_{\text{in}} \cup \Gamma_{\text{out}})}$  and  $\Gamma_{\text{out}} := (\{x = 2.2\} \cap \partial\Omega) \setminus \partial(\{x = 2.2\} \cap \partial\Omega)$ . Furthermore, the viscosity  $\nu = 10^{-3}$  and  $u_{\text{in}}(x, y) = (0.3w(y), 0)$  with  $w(y) = 4y(H - y)/H^2$  and  $H = 0.41$ . The corresponding weak form reads as follows: Find  $\vec{u} = (u, p) \in V_{BC} := [H^1(\Omega)]_{BC}^2 \times L^2(\Omega)$  such that

$$A(\vec{u})(\vec{v}) = 0 \quad \forall \vec{v} = (v_u, v_p) \in V_0 := [H_0^1(\Omega)]^2 \times L^2(\Omega) \quad (1)$$

with

$$\begin{aligned} A(\vec{u})(\vec{v}) := & (\nu(\nabla u + \nabla u^T), \nabla v_u)_{[L^2(\Omega)]^{2 \times 2}} + ((u \cdot \nabla)u, v_u)_{[L^2(\Omega)]^2} \\ & + (p, \operatorname{div}(v_u))_{L^2(\Omega)} - (\operatorname{div}(u), v_p)_{L^2(\Omega)}, \end{aligned}$$

where  $[H^1(\Omega)]_{BC}^2 := \{u \in [H^1(\Omega)]^2 : u|_{\Gamma_{\text{in}}} = u_{\text{in}} \wedge u|_{\Gamma_{\text{no-slip}}} = 0\}$  and  $[H_0^1(\Omega)]^2 := \{v \in [H^1(\Omega)]^2 : v|_{\Gamma_{\text{in}}} = 0 \wedge v|_{\Gamma_{\text{no-slip}}} = 0\}$ .



Figure 1: The computational domain  $\Omega$  (left) and the initial mesh (right).

### 2.2 Discretization

Let  $\mathcal{T}_h$  be a decomposition of  $\Omega \subset \mathbb{R}^2$  into quadrilateral elements. Furthermore, we assume that  $\mathcal{T}_{\frac{h}{2}}$  is the uniform refinement of  $\mathcal{T}_h$ . We discretize our problem using  $[Q_c^2]^2$ , i.e. piecewise bi-quadratic elements for the velocity  $u$ , and  $Q_c^1$ , i.e. piecewise bi-linear elements for the pressure  $p$ . The resulting space using the mesh  $\mathcal{T}_h$  will be denoted by  $V_h$ . For a more detailed explanation of the discretization, we refer to [4]. The resulting space using the mesh  $\mathcal{T}_{\frac{h}{2}}$  will be denoted by  $V_{\frac{h}{2}}$ . We say  $V_{\frac{h}{2}}$  is the (hierarchical)  $h$ -refined finite element space of  $V_h$ . Furthermore we consider using  $[Q_c^4]^2$ , i.e. piecewise bi-quartic elements for the velocity  $u$ , and  $Q_c^2$ , i.e. piecewise bi-quadratic elements

for the pressure  $p$ . The resulting finite element space using the mesh  $\mathcal{T}_h$  will be denoted by  $V_h^{(2)}$ . Here we have the property that  $V_h \subset V_h^{(2)}$ . We say  $V_h^{(2)}$  is the (hierarchical)  $p$ -refined finite element space of  $V_h$ . The corresponding discretized problems read as: Find  $\vec{u}_h \in V_h \cap V_{BC}$ ,  $\vec{u}_{\frac{h}{2}} \in V_{\frac{h}{2}} \cap V_{BC}$  and  $\vec{u}_h^{(2)} \in V_h^{(2)} \cap V_{BC}$  such that

$$\begin{aligned} A(\vec{u}_h)(\vec{v}_h) &= 0 & \forall \vec{v}_h \in V_h \cap V_0, \\ A(\vec{u}_{\frac{h}{2}})(\vec{v}_{\frac{h}{2}}) &= 0 & \forall \vec{v}_{\frac{h}{2}} \in V_{\frac{h}{2}} \cap V_0, \\ A(\vec{u}_h^{(2)})(\vec{v}_h^{(2)}) &= 0 & \forall \vec{v}_h^{(2)} \in V_h^{(2)} \cap V_0. \end{aligned}$$

**Remark 2.1.** *We would like to mention that the domain  $\Omega$  is not of polygonal shape. Therefore, a decomposition into quadrilateral elements is not possible. However, we approximate the ball  $B$  by a polygonal domain, which is adapted after every refinement process by describing it as a spherical manifold in deal.II [1] using the command `Triangulation::set_manifold`.*

### 3 Dual Weighted Residual Method and Error Representation

We are primarily interested in one or more particular quantities of interest. We employ the dual weighted residual (DWR) method [2] for estimating the error in these quantities. To connect the quantity of interest  $J$  with the model problem, we consider the adjoint problem.

#### 3.1 The Adjoint Problem

The adjoint problem reads as follows: Find  $\vec{z} \in V_0$  such that

$$A'(\vec{u})(\vec{v}, \vec{z}) = J'(\vec{u})(\vec{v}) \quad \forall \vec{v} \in V_0, \quad (2)$$

where  $A'$  and  $J'$  denote the Frechet derivative of  $A$  and  $J$ , respectively, and  $\vec{u}$  is the solution of the model problem (1).

**Theorem 3.1.** *Let us assume that  $J \in \mathcal{C}^3(V_{BC}, \mathbb{R})$ . If  $\vec{u}$  solves the model problem (1) and  $\vec{z}$  solves the adjoint problem (2), then, for arbitrary fixed  $\vec{u} \in V_{BC}$  and  $\vec{z} \in V_0$ , the following error representation formula holds:*

$$\begin{aligned} J(\vec{u}) - J(\vec{u}) &= \frac{1}{2} \rho(\vec{u})(\vec{z} - \vec{z}) + \frac{1}{2} \rho^*(\vec{u}, \vec{z})(\vec{u} - \vec{u}) + \rho(\vec{u})(\vec{z}) + \mathcal{R}^{(3)}, \\ \text{where } \rho(\vec{u})(\cdot) &:= -A(\vec{u})(\cdot), \quad \rho^*(\vec{u}, \vec{z})(\cdot) := J'(\vec{u})(\cdot) - A'(\vec{u})(\cdot, \vec{z}), \text{ and} \\ \mathcal{R}^{(3)} &:= \frac{1}{2} \int_0^1 [J'''(\vec{u} + s\vec{e})(\vec{e}, \vec{e}, \vec{e}) - A'''(\vec{u} + s\vec{e})(\vec{e}, \vec{e}, \vec{e}, \vec{z} + s\vec{e}^*) - 3A''(\vec{u} + s\vec{e})(\vec{e}, \vec{e}, \vec{e}^*)] s(s-1) ds, \\ &\text{with } \vec{e} = \vec{u} - \vec{u} \text{ and } \vec{e}^* = \vec{z} - \vec{z}. \end{aligned} \quad (3)$$

*Proof.* We refer the reader to [3] and [12]. □

**Remark 3.2.** *In practice, the arbitrary elements  $\vec{u} \in V_{BC}$  and  $\vec{z} \in V_0$  will be replaced by approximations  $\vec{u}_h$  and  $\vec{z}_h$  to the corresponding finite element solutions.*

**Remark 3.3.** *The error representation formula in Theorem 3.1 is exact but not computable, because  $\vec{u}$  and  $\vec{z}$  are not known.*

### 3.2 Error Estimation and Adaptive Algorithm

The different error estimator parts are discussed in [4]. In particular, it turns out that  $\eta_h := \frac{1}{2}\rho(\vec{u})(\vec{z} - \vec{z}) + \frac{1}{2}\rho^*(\vec{u}, \vec{z})(\vec{u} - \vec{u})$  is related to the discretization error [12, 3, 4]. The idea is to replace the quantities  $\vec{u} - \vec{u}$  and  $\vec{z} - \vec{z}$  by some computable quantities. This can be done via higher order interpolation [2, 12] or hierarchically (via an additional solve on an enriched space) [2, 3, 10]. If  $u_h^+$ ,  $z_h^+$  are the solution, then we approximate  $\vec{u} - \vec{u}$  and  $\vec{z} - \vec{z}$  by  $u_h^+ - \vec{u}$  and  $z_h^+ - \vec{z}$ , respectively. The new computable error estimator then reads as

$$\eta_h^+ := \frac{1}{2}\rho(\vec{u})(z_h^+ - \vec{z}) + \frac{1}{2}\rho^*(\vec{u}, \vec{z})(u_h^+ - \vec{u}).$$

Under some saturation assumption, it was shown in [4] that the resulting error estimator is efficient and reliable. We consider the two different error estimators

$$\begin{aligned} \eta_h^{(2)} &:= \frac{1}{2}\rho(\vec{u})(z_h^{(2)} - \vec{z}) + \frac{1}{2}\rho^*(\vec{u}, \vec{z})(u_h^{(2)} - \vec{u}), \\ \eta_{\frac{h}{2}} &:= \frac{1}{2}\rho(\vec{u})(z_{\frac{h}{2}} - \vec{z}) + \frac{1}{2}\rho^*(\vec{u}, \vec{z})(u_{\frac{h}{2}} - \vec{u}). \end{aligned}$$

We call  $\eta_h^{(2)}$  and  $\eta_{\frac{h}{2}}$  the  $p$ -enriched and  $h$ -enriched error estimators, respectively. The error estimators are localized using the partition of unity technique proposed in [13]. The marking strategy and algorithms are the same as in [4].

**Remark 3.4.** *The efficiency and reliability are not guaranteed under the corresponding saturation assumption in [4] for  $\eta_{\frac{h}{2}}$ , since the boundary is adapted in every refinement step.*

**Remark 3.5.** *We use the algorithm presented in [4]. The algorithm using  $p$  enrichment coincides with Algorithm 3 in [4]. In the algorithm, where we use  $h$  enrichment, we replace  $V_h^{(2)}$  by  $V_{\frac{h}{2}}$ .*

## 4 Numerical Experiment

We compare the two error estimators introduced in Section 3.2. In the  $p$  enriched case, we use uniform  $p$  refinement for the hierarchical approximation. The results for  $p$  enrichment have already been computed in [4]. In the  $h$  enriched case, we use uniform  $h$  refinement. The configuration of the problem is given in Section 2.1.

## 4.1 Quantities of Interest

We use the quantities of interest defined in [14, 4]:

$$\begin{aligned}\Delta p(\vec{u}) &:= p(X_1) - p(X_2), \\ c_{\text{drag}}(\vec{u}) &:= C \int_{\partial B} [\nu(\nabla u + \nabla u^T)\vec{n} - p\vec{n}] \cdot \vec{e}_1 \, ds_{(x,y)}, \\ c_{\text{lift}}(\vec{u}) &:= C \int_{\partial B} [\nu(\nabla u + \nabla u^T)\vec{n} - p\vec{n}] \cdot \vec{e}_2 \, ds_{(x,y)},\end{aligned}$$

where  $C = 500$ ,  $X_1 = (0.15, 0.2)$ ,  $X_2 = (0.25, 0.2)$ ,  $\vec{e}_1 := (1, 0)$ ,  $\vec{e}_2 := (0, 1)$ , and  $\vec{n}$  denotes the outer normal vector. To do adaptivity for all of them at once we combine them to one functional

$$J_{\mathfrak{E}}(\vec{v}_h) := \frac{|\Delta p(\vec{u}_h^+ - \vec{v}_h)|}{|\Delta p(\vec{u}_h)|} + \frac{|c_{\text{drag}}(\vec{u}_h^+ - \vec{v}_h)|}{|c_{\text{drag}}(\vec{u}_h)|} + \frac{|c_{\text{lift}}(\vec{u}_h^+ - \vec{v}_h)|}{|c_{\text{lift}}(\vec{u}_h)|}.$$

By  $J_{\mathfrak{E}}^p$  or  $J_{\mathfrak{E}}^h$ , we denote the functionals where we replace  $\vec{u}_h^+$  with  $\vec{u}_h^{(2)}$  or  $\vec{u}_{\frac{h}{2}}$ , respectively. More information on how to treat multiple functionals at once can be found in [8, 7, 15, 11, 9, 5, 3, 4]. The implementation is done in the finite element library `deal.II` [1], and follows the code in [4]. In this section, we compare two different sequences of meshes. The sequences are generated by the error estimators  $\eta_h^{(2)}$  and  $\eta_{\frac{h}{2}}$ . First of all, let us define the effectivity indices by

$$I_{eff}^p := \frac{\eta_h^{(2)}}{|J_{\mathfrak{E}}^p(u) - J_{\mathfrak{E}}^p(u_h)|} \quad \text{and} \quad I_{eff}^h := \frac{\eta_{\frac{h}{2}}}{|J_{\mathfrak{E}}^h(u) - J_{\mathfrak{E}}^h(u_h)|}.$$

The  $p$  enriched discrete remainder part of the error estimator  $\eta_{\mathcal{R}}^{(2)}$  is defined as the quantity (3), where we replace  $\vec{u}, \vec{z}, \vec{u}, \vec{z}$  by  $\vec{u}_h, \vec{z}_h, \vec{u}_h^{(2)}, \vec{z}_h^{(2)}$ , respectively. The  $h$  enriched discrete remainder part of the error estimator  $\eta_{\mathcal{R}, \frac{h}{2}}$  is defined as the quantity (3), where we replace  $\vec{u}, \vec{z}, \vec{u}, \vec{z}$  by  $\vec{u}_h, \vec{z}_h, \vec{u}_{\frac{h}{2}}, \vec{z}_{\frac{h}{2}}$ , respectively. Finally, we define the gaps between the theoretical findings in [4] by

$$\eta_{\mathbb{E}}^{(2)} := \left| |J(\vec{u}_h^{(2)}) - J(\vec{u}_h)| - |\eta_h^{(2)} + \rho(\vec{u}_h, \vec{z}_h) + \eta_{\mathcal{R}}^{(2)}| \right|,$$

and

$$\eta_{\mathbb{E}, \frac{h}{2}} := \left| |J(\vec{u}_{\frac{h}{2}}) - J(\vec{u}_h)| - |\eta_{\frac{h}{2}} + \rho(\vec{u}_h, \vec{z}_h) + \eta_{\mathcal{R}, \frac{h}{2}}| \right|.$$

## 4.2 Discussion of the Results

In Figure 2, the effectivity indices for the two different types of error estimators are shown on their respective grids. We see that  $h$ -enrichment delivers effectivity indices which are very close to one, whereas for  $p$ -enrichment we have effectivity indices in the range of  $0.2 - 8.1$ . This was also observed in [4]. In the case of  $p$ -enrichment, the saturation assumption is violated multiple times, as we observe in Figure 3. The saturation assumption is violated if the error  $|J_{\mathfrak{E}}^p(\vec{u}_h^{(2)}) - J_{\mathfrak{E}}^p(\vec{u})|$  in the enriched solution is larger than  $|J_{\mathfrak{E}}^p(\vec{u}_h) - J_{\mathfrak{E}}^p(\vec{u})|$ . In the case of  $h$ -enrichment, this always happens. If we compare the errors of the single

functionals, which are monitored in Figure 4, Figure 5 and Figure 6, we conclude that the meshes generated by the  $p$ -enriched error estimator lead to smaller errors in the single functionals. If all the conditions in [4] are fulfilled, then  $\eta_{\mathbb{E}}^{(2)}$  and  $\eta_{\mathbb{E}, \frac{h}{2}}$  are zero. However, in the computation of the error estimators, our overall round-off error is in the order of  $\varepsilon(\text{double}) \times \text{DOFs}$ , where  $\varepsilon(\text{double}) = 2^{-52}$  is the machine precision for double floating point numbers<sup>1</sup>. In the case of  $p$  enrichment, we observe in Figure 7 that  $\eta_{\mathbb{E}}^{(2)}$  indeed is in the order or even better than the round off errors when summing up the different error contributions. In this case, all requirements are fulfilled. For  $h$  enrichment, we do not have the inclusion  $V_h \subset V_{\frac{h}{2}}$  due to the geometrical approximation. Therefore, these conditions are violated. The effects are monitored in Figure 7 as well. The quantity  $\eta_{\mathbb{E}, \frac{h}{2}}$  does not only contain numerical round off errors, but also errors coming from the geometrical approximation. However, this is a non-local quantity, and the localization is not straightforward.

---

<sup>1</sup>[https://en.wikipedia.org/wiki/Machine\\_epsilon](https://en.wikipedia.org/wiki/Machine_epsilon)

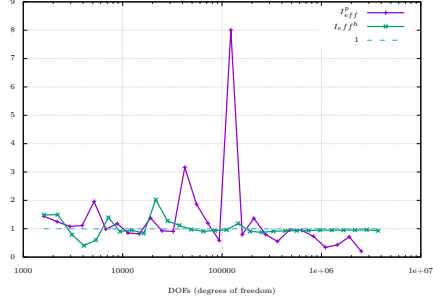


Figure 2: The two effectiveness indices on the corresponding meshes.

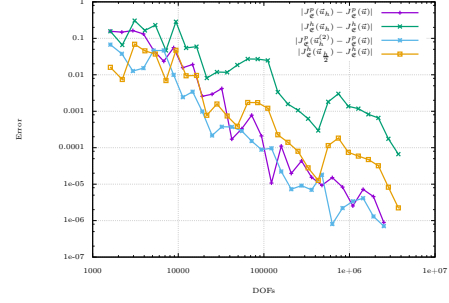


Figure 3: Errors in  $J_{\mathcal{E}}^p$  and  $J_{\mathcal{E}}^h$  in the solution and enriched solution.

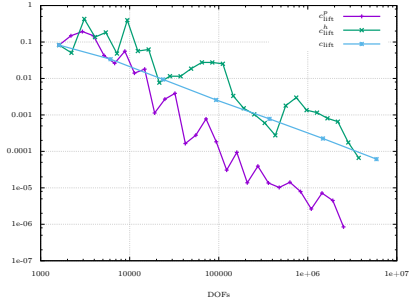


Figure 4: The errors in  $c_{lift}$  for refinement with  $p$ -enriched error estimation ( $c_{lift}^p$ ), refinement with  $h$ -enriched error estimation ( $c_{lift}^h$ ), and uniform refinement ( $c_{lift}$ ).

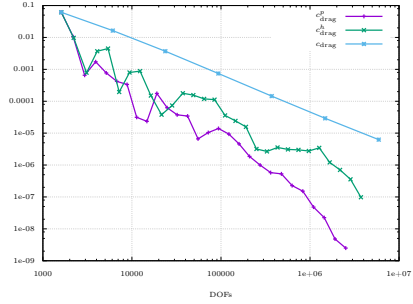


Figure 5: The errors in  $c_{drag}$  for refinement with  $p$ -enriched error estimation ( $c_{drag}^p$ ), refinement with  $h$ -enriched error estimation ( $c_{drag}^h$ ), and uniform refinement ( $c_{drag}$ ).

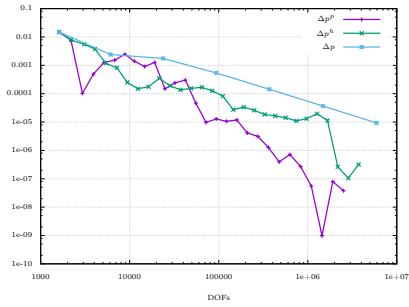


Figure 6: The errors in  $\Delta p$  for refinement with  $p$ -enriched error estimation ( $\Delta p^p$ ), refinement with  $h$ -enriched error estimation ( $\Delta p^h$ ), and uniform refinement ( $\Delta p$ ).

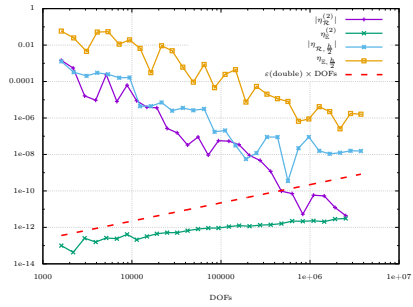


Figure 7: The remainder parts  $\eta_{\mathcal{R}}^{(2)}$ ,  $\eta_{\mathcal{R}, \frac{h}{2}}^{(2)}$  and gap parts  $\eta_{\mathbb{E}}^{(2)}$ ,  $\eta_{\mathbb{E}, \frac{h}{2}}^{(2)}$  for  $p$  and  $h$  enrichment. The remainder parts  $\eta_{\mathcal{R}}^{(2)}$ ,  $\eta_{\mathcal{R}, \frac{h}{2}}^{(2)}$  are indeed neglectable as usually done in literature.

## Acknowledgement

This work has been supported by the Austrian Science Fund (FWF) under the grant P 29181 ‘Goal-Oriented Error Control for Phase-Field Fracture Coupled to Multiphysics Problems’. Furthermore, we thank Daniel Jodlbauer for discussions.

## References

- [1] G. Alzetta, D. Arndt, W. Bangerth, V. Boddu, B. Brands, D. Davydov, R. Gassmüller, T. Heister, L. Heltai, K. Kornmann, M. Kronbichler, M. Maier, J.-P. Pelteret, B. Turcksin, and D. Wells. The `deal.II` library, version 9.0. *J. Numer. Math.*, 26(4):173–183, 2018.
- [2] R. Becker and R. Rannacher. An optimal control approach to a posteriori error estimation in finite element methods. *Acta Numer.*, 10:1–102, 2001.
- [3] B. Endtmayer, U. Langer, and T. Wick. Multigoal-oriented error estimates for non-linear problems. *J. Numer. Math.*, 2018, DOI: 10.1515/jnma-2018-0038. published online.
- [4] B. Endtmayer, U. Langer, and T. Wick. Two-side a posteriori error estimates for the DWR method. *SIAM J. Sci. Comput.*, 2019. accepted.
- [5] B. Endtmayer and T. Wick. A Partition-of-Unity Dual-Weighted Residual Approach for Multi-Objective Goal Functional Error Estimation Applied to Elliptic Problems. *Comput. Methods Appl. Math.*, 17(4):575–599, 2017.
- [6] V. Girault and P.-A. Raviart. *Finite Element method for the Navier-Stokes equations*. Number 5 in Computer Series in Computational Mathematics. Springer-Verlag, 1986.
- [7] R. Hartmann. Multitarget error estimation and adaptivity in aerodynamic flow simulations. *SIAM J. Sci. Comput.*, 31(1):708–731, 2008.
- [8] R. Hartmann and P. Houston. Goal-oriented a posteriori error estimation for multiple target functionals. In *Hyperbolic problems: theory, numerics, applications*, pages 579–588. Springer, Berlin, 2003.
- [9] K. Kergrene, S. Prudhomme, L. Chamoin, and M. Laforest. A new goal-oriented formulation of the finite element method. *Comput. Methods Appl. Mech. Engrg.*, 327:256–276, 2017.
- [10] U. Köcher, M. P. Bruchhäuser, and M. Bause. Efficient and scalable data structures and algorithms for goal-oriented adaptivity of space-time FEM codes. *SoftwareX*, 10:100239, 2019.
- [11] D. Pardo. Multigoal-oriented adaptivity for hp-finite element methods. *Procedia Computer Science*, 1(1):1953 – 1961, 2010.



- [12] R. Rannacher and J. Vihharev. Adaptive finite element analysis of nonlinear problems: balancing of discretization and iteration errors. *J. Numer. Math.*, 21(1):23–61, 2013.
- [13] T. Richter and T. Wick. Variational localizations of the dual weighted residual estimator. *J. Comput. Appl. Math.*, 279:192–208, 2015.
- [14] M. Schäfer, S. Turek, F. Durst, E. Krause, and R. Rannacher. Benchmark computations of laminar flow around a cylinder. In *Flow simulation with high-performance computers II*, pages 547–566. Springer, 1996.
- [15] E. H. van Brummelen, S. Zhuk, and G. J. van Zwieten. Worst-case multi-objective error estimation and adaptivity. *Comput. Methods Appl. Mech. Engrg.*, 313:723–743, 2017.